

Final Project: Dielectric Spectroscopy with the NanoVNA2

The code and raw data for this project live [here](#).

The project development documentation lives [here](#).

Motivation

Though dielectric spectroscopy would appear limited to characterizing a material's dielectric properties, it is a useful tool in a diverse set of applications as many other material properties can be related to dielectric properties [1]. Example industrial applications include determining chemical behaviors of food products or bacterial contamination [2]. As shown in the Agilent Technologies tech note on dielectric spectroscopy (Figure 1), the real permittivity of milk measurably changes as it approaches spoilage [2].

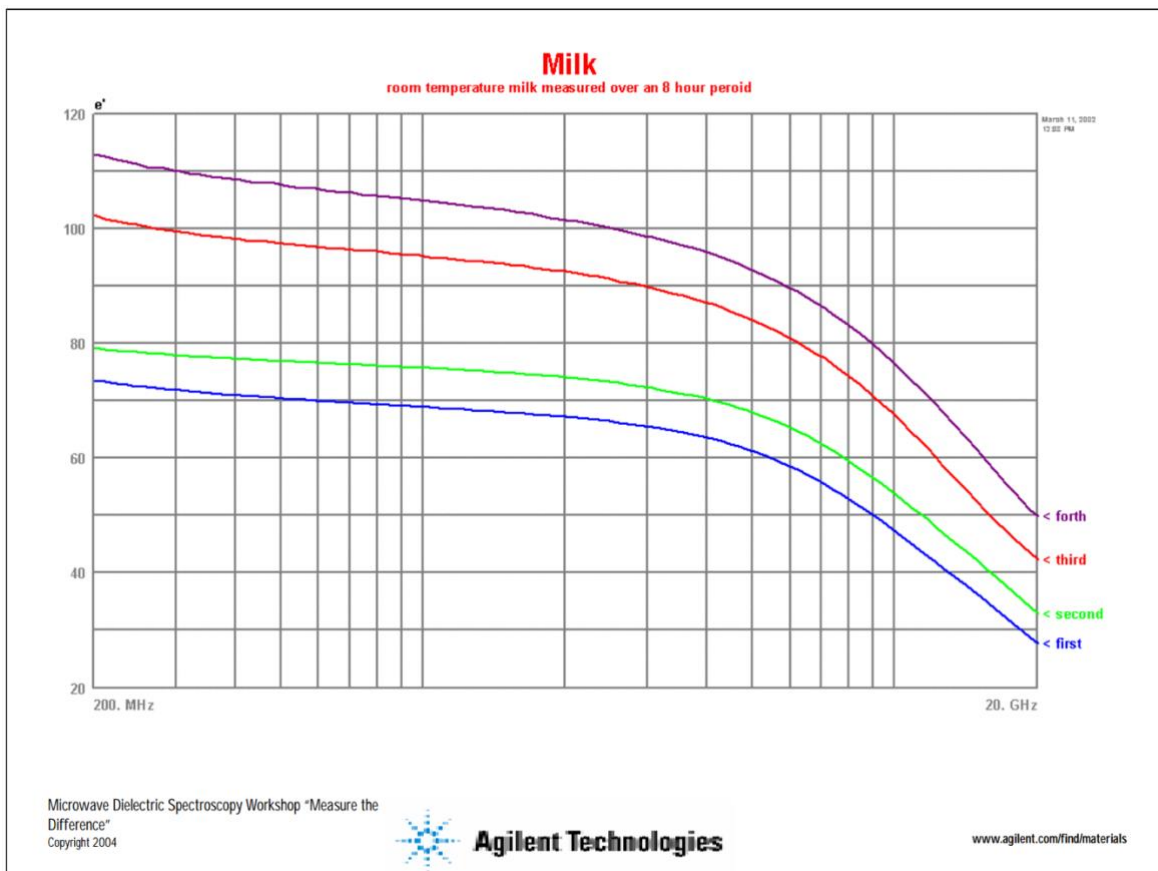


Figure 1 — Agilent tech note graph of the real permittivity of milk. [Source](#) [2].

(Dielectric properties are also interesting in their own right, beyond applications to food. [3] boldly asserts that broadband dielectric spectroscopy should one day compete with infrared spectroscopy and nuclear magnetic resonance in its publication amount).

The experimental set up for dielectric spectroscopy requires expensive lab equipment, which limits its wider use. Agilent (now Keysight) vector network analyzers run from >\$3k used to \$10-100k new (e.g., [handheld analyzer](#), [ENA VNA](#)). The additional testing equipment required (probes, fixturing) can also run on the order of \$10k additional cost.

Very cheap VNAs have (somewhat) recently come on the scene, such as the [NanoVNA SAA-2N V2.2](#) which runs for \$130 on Amazon (and also maintains extensive [documentation](#)). So, this projects asks: Can we do dielectric spectroscopy at the ~fablab-able scale?



Figure 2 — NanoVNA. [From Amazon listing](#).

Background

We have the constitutive relations:

$$D = \epsilon E$$

And

$$B = \mu H$$

Where ϵ and μ are the electrical permittivity and magnetic permeability, respectively. These parameters describe the way fields interact with materials. In DC land, these can both be treated as constants. As frequency increases, this no longer holds.

The relative complex permittivity is given by:

$$\epsilon_r = \epsilon' - j\epsilon''$$

Where ϵ' (the real part of the permittivity) describes the material's ability to store electric field (in DC, the dielectric constant), and ϵ'' is the loss factor and describes the energy loss. (ϵ'' is responsible for how microwave ovens cook).

The relationship between complex permittivity and frequency is illustrated in Fig. 3.

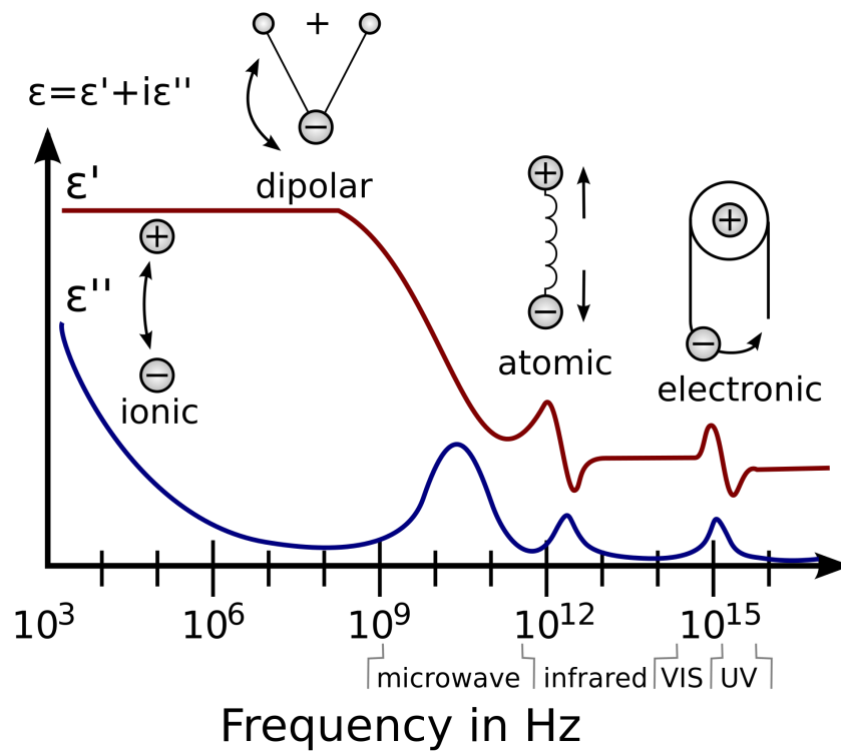


Figure 3 — relative complex permittivity mechanisms as a function of frequency [1]. [Image source.](#)

Let's consider dipolar relaxation since if we are able to see any interesting behavior, it will likely be dominated by these effects. For an ideal distribution of non-interacting dipoles, the permittivity is described using Debye relaxation, which gives [4]:

$$\epsilon' = \epsilon_\infty + \frac{\epsilon_s - \epsilon_\infty}{1 + \omega^2\tau^2}$$

$$\epsilon'' = \frac{(\epsilon_s - \epsilon_\infty)\omega\tau}{1 + \omega^2\tau^2}$$

Where ϵ_s is the static permittivity (what we think of as the dielectric constant in DC), ϵ_∞ is the upper limit of the frequency (what ϵ' approaches in the above figure), and τ is the relaxation time.

Using these equations, we can plot the ideal responses for various materials. Given what I will test, let's plot DI water and ethanol (see Fig. 4 and Fig. 5). The material parameters are from [5].

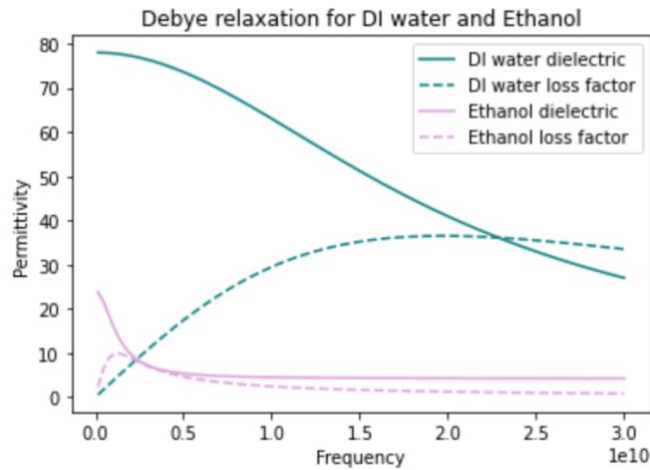


Figure 4 — The permittivity of DI water and ethanol from 0.1-30GHz. Solid line is ϵ' and dashed line is ϵ'' .

We won't be able to measure for this range though, so let's plot just the range 1.5-3GHz.

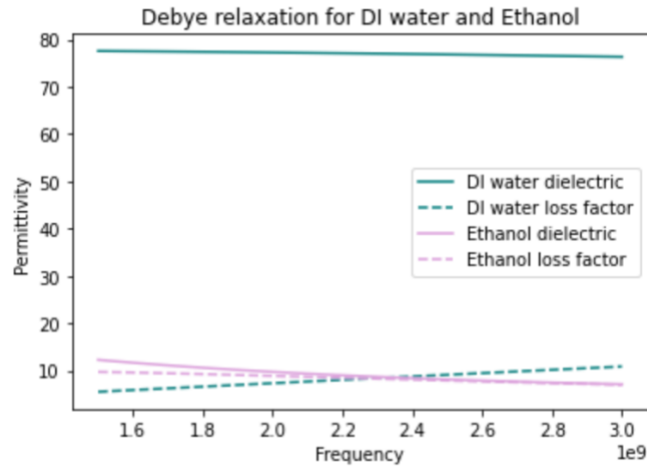


Figure 5 — The permittivity of DI water and ethanol from 1.5-3GHz. Solid line is ϵ' and dashed line is ϵ'' .

As you can see, there aren't any particularly dramatic changes in this region, so please begin to scale your expectations appropriately for the following sections.

Overview

I will use free-space dielectric spectroscopy for this project. The apparatus for this consists of two horn antennas with a material under test (MUT) between them, and a VNA measuring the transmissivity between the antennas. This is illustrated in Fig. 6, from [1].

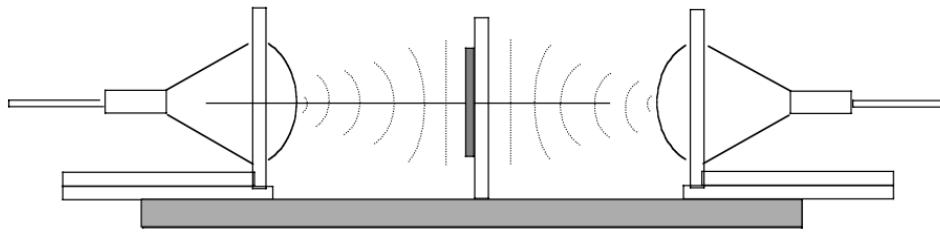
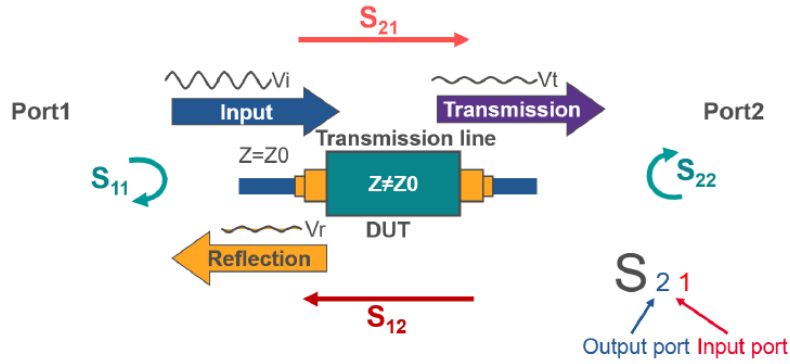


Figure 6 — Free space measurement set up. [Source](#)

The advantages to this design include flexibility in the type/shape and temperature of the material under test, and that it is fairly broadband. However, as we will soon see, in the lower frequency range, the horn antenna size is a limiting factor and given this, it may have made more practical sense to pick a different testing set up, such as a coaxial probe or even a capacitive plate design. Anyways, this is what Neil encouraged me to do, so here we are.

From this testing apparatus, our collected data consists of S-parameter data, which describes the transmission/reflection of signals in the system. We then have to extract permittivity (and permeability, if you're so inclined) from that. To recap nomenclature, Fig. 7 from [6] is a useful illustration.



Reflection/Input = Reflection coefficient $\rightarrow S_{11}, S_{22}$

Transmission/Input = Transmission coefficient $\rightarrow S_{21}, S_{12}$

Figure 7 — S-parameter illustration. [Source](#) [6].

Experimental design

3D printed horn antennas

Prior to thinking deeply about the frequency range of our VNA, I made a pair of Ka-band horn antennas according to procedure given by the [Antenna Test Lab](#) [7].

[7] Gives very detailed documentation on the process of producing 3D printed horn antennas with comparable performance to commercial versions. The print file is made using the manufacturer provided CAD model for the antenna and printed on a standard FDM printer. In this case, I used PLA filament on a Prusa. The surface is then smoothed. The reference uses chemical smoothing or sanding. Since I used PLA, I sanded the horn down. The difference between a smoothed and unsmoothed print is shown in Fig. 8.

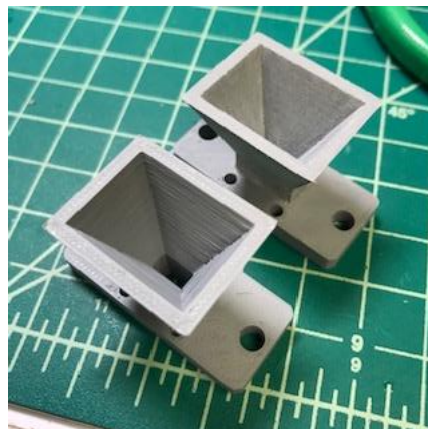


Figure 8 – raw print and smoothed print.

The antennas are then painted with a conductive spray paint. I used [MG chemicals spray on paint](#).

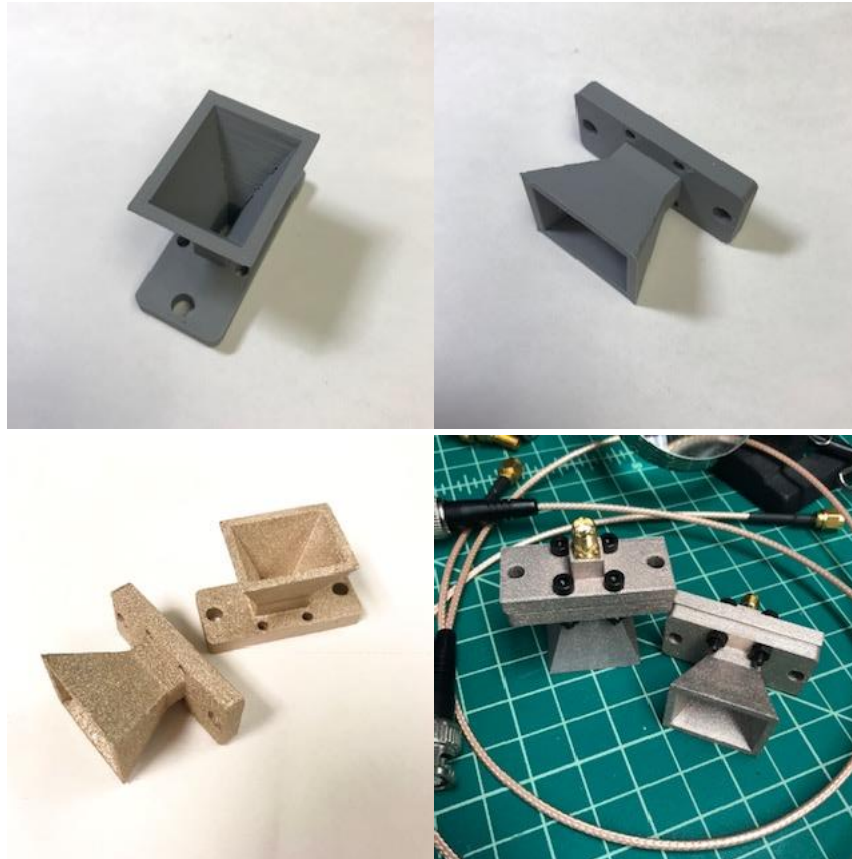


Figure 9 – 3D printed horn antennas

I made the SMA-to-antenna launch in the same fashion. I found a commercial inline launch model and adapted it to fit the SMA ends we had. The final horns are shown in Fig. 9. Upon trying them out with the VNA, I realized that these are for a frequency range an order of magnitude above the maximum of the VNA. So, there was no wave propagation.

Laser cut horn antennas

To pick reasonable waveguide dimensions, we should know the wavelengths that we'll be sweeping through. Let's say we want to go from 1GHz to 3GHz:

$$\lambda_{1GHz} = \frac{c}{\nu} = \frac{3 \times 10^8}{1 \times 10^9} = 3 \times 10^{-1}[m]$$

$$\lambda_{3GHz} = \frac{c}{\nu} = \frac{3 \times 10^8}{3 \times 10^9} = 1 \times 10^{-1}[m]$$

From [here](#) [], the cutoff frequency is given by:

$$\omega_c = \frac{1}{\sqrt{\mu\epsilon}} \sqrt{\left(\frac{m\pi}{a}\right)^2 + \left(\frac{n\pi}{w}\right)^2}$$

Where a and w are the side lengths of the rectangular waveguide and (m, n) are the mode numbers. There are then additionally other heuristics and guiding equations at play for picking the correct dimensions, some of which are discussed here [8].

After fruitlessly exploring that, I abdicated responsibility and picked a commercial waveguide in the relevant frequency range: [WR430](#), which has a cutoff frequency of 1.362GHz for the lowest order mode and a recommended range of 1.7-2.6GHz.

With a commercial specification, I can then use the dimensions of a commercial product for the horn antenna. I picked [Pasternack's WR-430 Waveguide Standard Gain Horn Antenna Operating from 1.7 GHz to 2.6 GHz with a Nominal 15 dB Gain SMA Female Input](#), which goes for >\$3k. Their product image is shown in Fig. 10.



Figure 10 — The Pasternack horn antenna. [Source](#).

This horn is huge, massive even. The 3D printing strategy becomes less appealing at this scale, given that the model would have to be sectioned into separate prints and would still require sanding. So, I pivoted to a new process: laser cut panels out of acetal, tape on copper foil, and hold position with a 3D printed bracket. This is shown in Fig. 11. The antenna sides

were longer than the bed of the Trotec Speedy 100 Flexx, so I instead down-sized to half the length, which is closer to Pasternack's 10dB version of this horn (this is shown in the highlighted portions of Fig. 11).

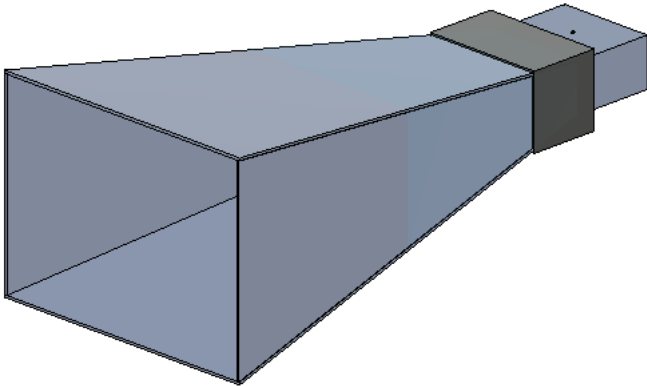


Figure 11 — CAD of WR430 horn modified for printing and cutting.

This still leaves some ambiguity about the placement and dimensions of the SMA launch. In the language of Fig. 12, the dimensions C and D are not fully decided by this.

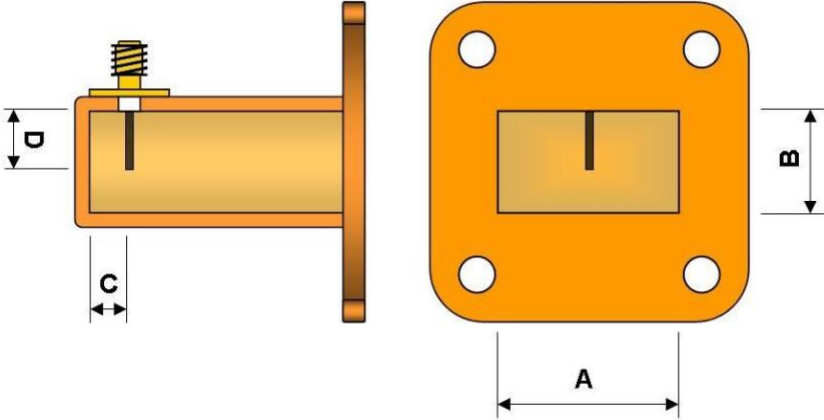


Figure 12 — SMA rectangular waveguide launch dimensions. [[Source](#)]

In practice, the dimension C is usually pre-set and using the heuristic:

$$C = \frac{\lambda}{4}$$

However, [8] suggests that this is not always ideal, with potentially smaller distances outperforming this spec. To this end, the back short of the horn can be adjusted. I did not find a good reference for the dimension D, so this was experimentally chosen based on a few lengths and the antenna pair's resulting transmission gain.

The complete horns are shown in Fig. 13.

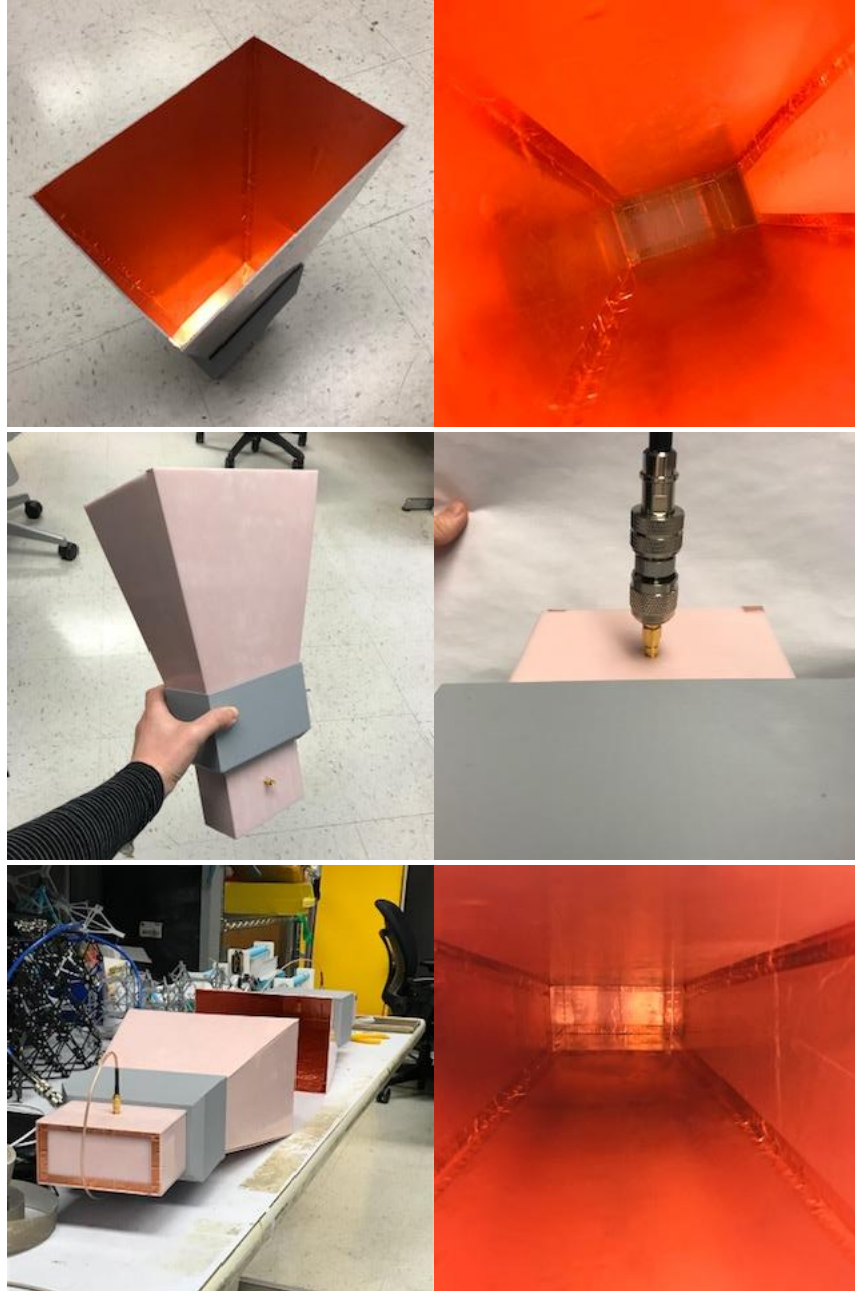


Figure 13 — Laser cut horn antennas.

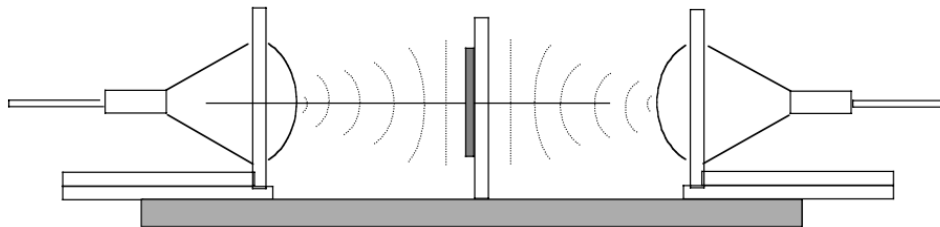


Figure 14 — Free space measurement set up. [Source](#).

Revisiting Fig. 14, the antennas are placed 24.5cm from each other. Their gain in dB is shown in Fig. 15 for the full range of the VNA and for the target range (magnitude S11 in blue and magnitude S21 in red).

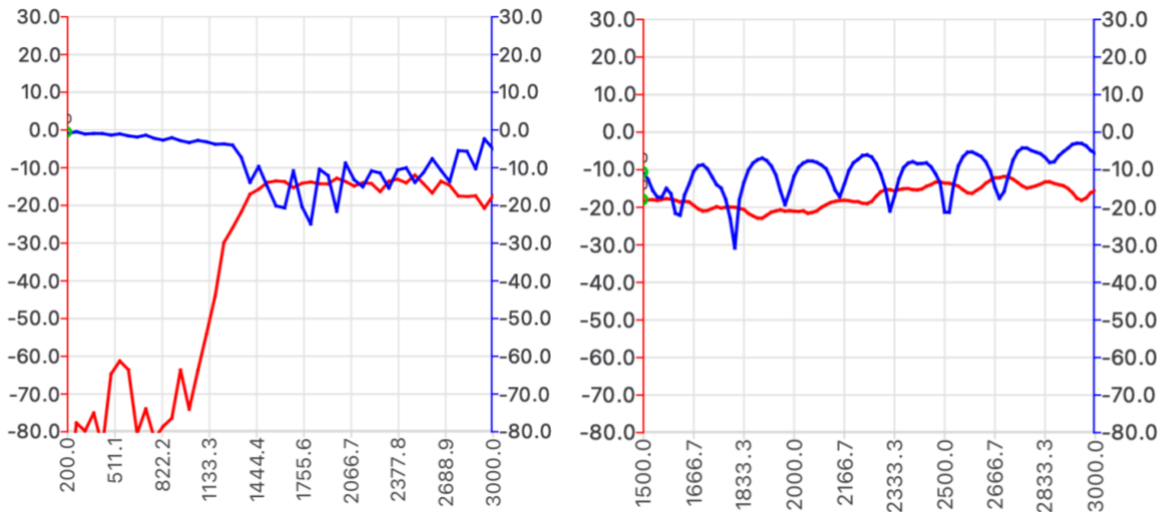


Figure 15 — (left) antenna gain from 200MHz to 3GHz. Blue line is S11 magnitude and red line is S21 magnitude. (right) antenna gain from 1.5GHz to 3GHz.

For fun, we can look at the antenna response using one of the fancy VNAs (Figure 16). (They look about the same.)



Figure 16 — S21 log magnitude for the antennas over the same frequency range.

Data acquisition

For planar materials (e.g., plastic sheet stock), the material is placed at the midpoint of the horns. For liquid materials, a plastic holder was made, consisting of acetal sheets glued together with a spacer to help maintain known thickness. This forms a flat container which

can be filled with liquids. Unfortunately, I used a very thin Delrin that results in some bulging in the sample holder, which contributes to systemic error.

Calibration

The VNA is calibrated using SOLT at the cable ends (no horns), using the standards given in the kit (Short, Open, Load, and Thru). The measurements were all taken with this calibration. For reference, see [9].

To calibrate out the testing set up (i.e., calibration plane between the antennas), there are a variety of calibration procedures, such as GRL, which Agilent has built in on some of their systems [2]. I am using TRL, or Through-Reflect-Line [10] because of its simplicity. For this, we first measure a Through standard, which consists of the antennas at the measurement distance with nothing between them. Next, we measure a reflect standard. TRL does not require a known reflectivity for this, only that the reflectivity is high. This is done using 3.16mm aluminum sheet placed at the midpoint between the antennas. The line standard is then a delay measurement. This is taken with the horn antennas offset by a quarter wavelength of the mid-band frequency, as recommended by [this](#). “Thru-Reflect-Line” is first described in [10], and a diagram from that paper is shown below for reference.

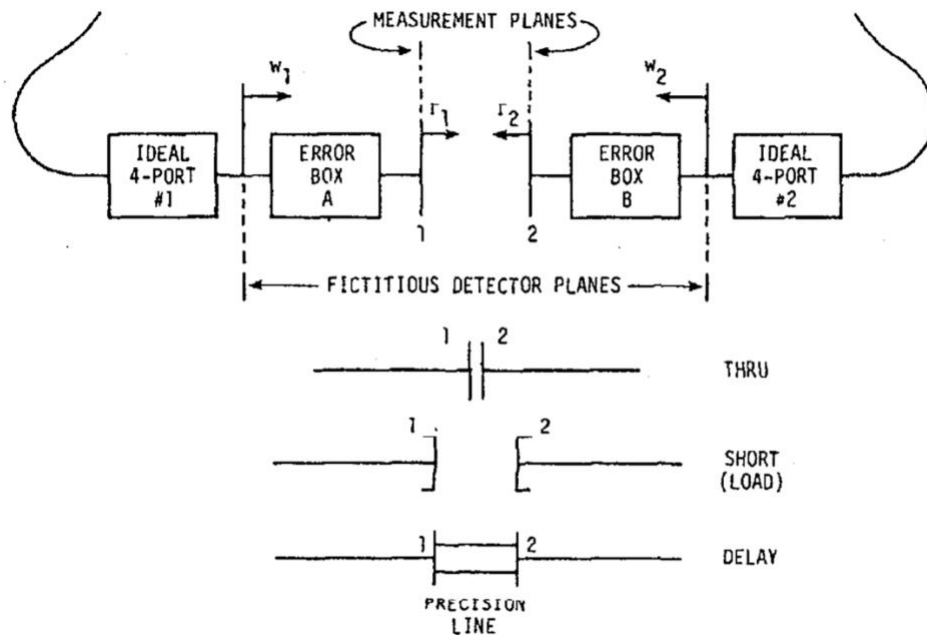


Figure 17— From [here](#). The measurement planes for TRL [10].

The TRL calibration is then implemented using [scikit-rf](#), a python library for RF/Microwave engineering [11]. After the TRL calibration, we can re-run our standards through the calibration to see how it looks. For the through standard, we expect 0dB for the transmission parameters and negative infinity dB for the reflectivity parameters. In practice, we get close to 0 dB for S21 and S12, and fairly negative gain for S11 and S22, which seems good. The results are shown in Fig. 18. Note that the NanoVNA2 is not a true 2 port network analyzer and it's not completely clear to me how it generates S22 and S12 parameters when it exports.

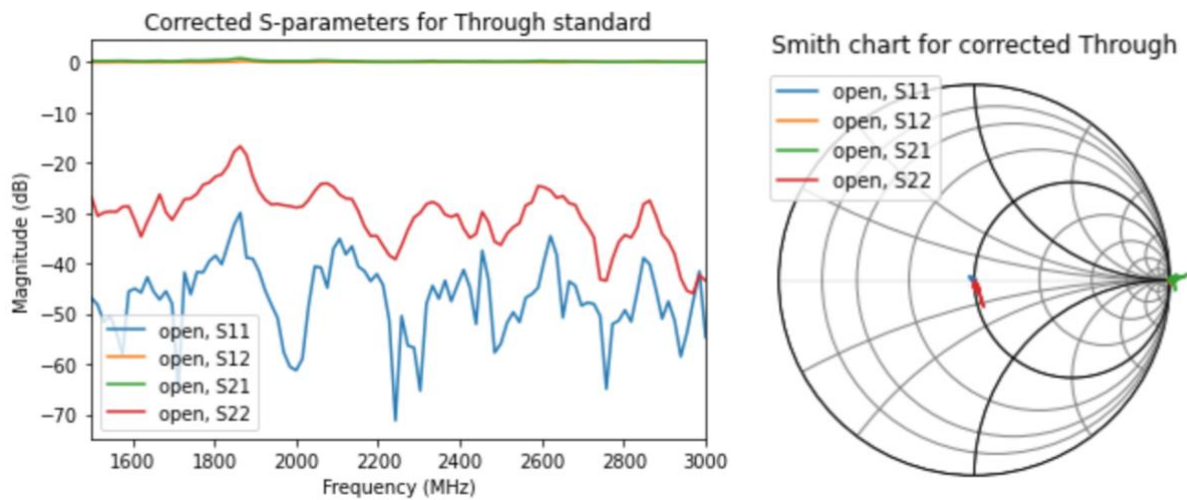


Figure 18 — Through standard after calibration.

The Reflect standard performs a bit worse. For this, we expect the opposite of the Through standard. That is, 0dB for the reflection parameters (S11 and S22) and negative infinity for the transmissions parameters (S21 and S12). This is not the case for the corrected S-parameters for the reflect standard, but I also don't think the results are terrible. The TRL calibration I used leaves out [switch terms](#) [11][12], which could improve the results.

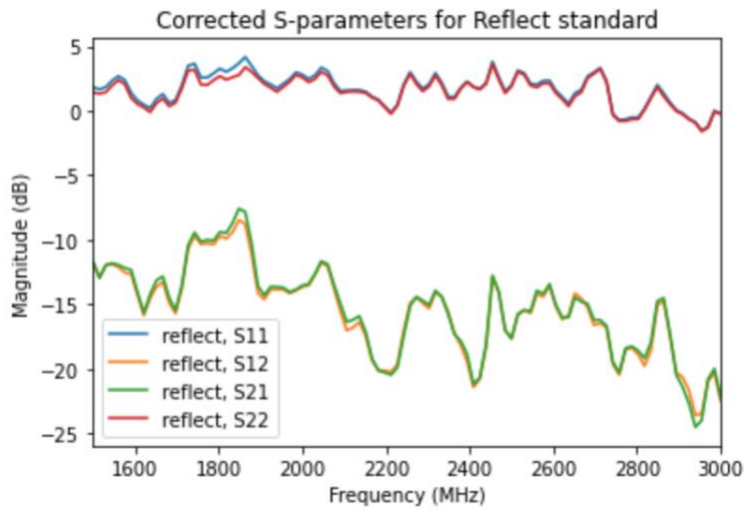


Figure 19 — Reflect standard after calibration.

For reference, here is a comparison of the raw S parameters for a 0.16mm copper sheet and the corrected S parameters (see Fig. 20). This will look a lot like the Reflect standard, since both of these are high reflectivity materials.

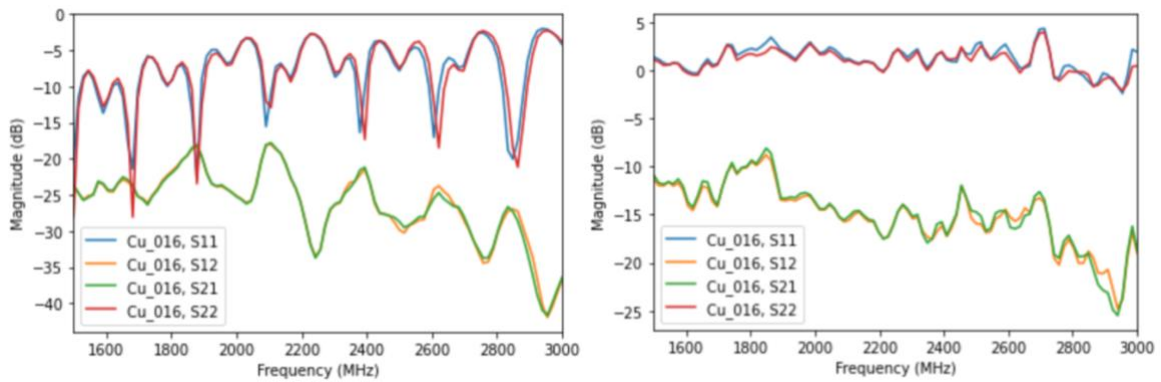


Figure 20 — Uncorrected (left) and corrected (right) S-parameters for a copper sheet.

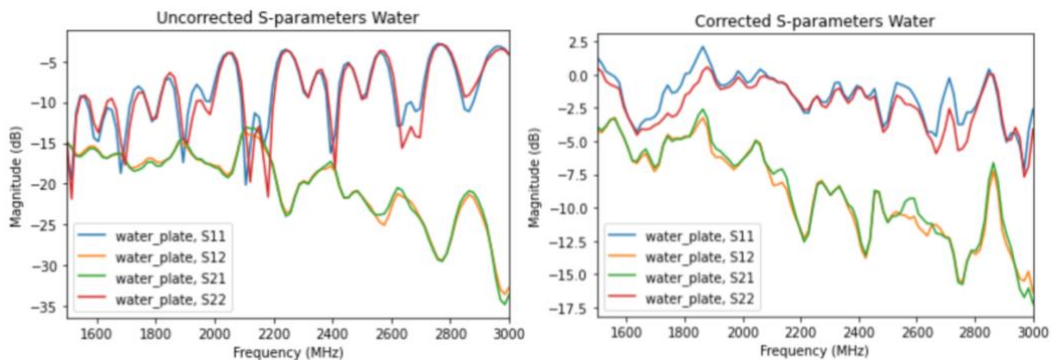


Figure 21 — Uncorrected and corrected parameters for tap water sample.

The uncorrected and corrected S-parameters for a tap water sample are shown. There is an amount of noise that appears to be introduced by the TRL calibration which may be a problem.

Extraction of permittivity

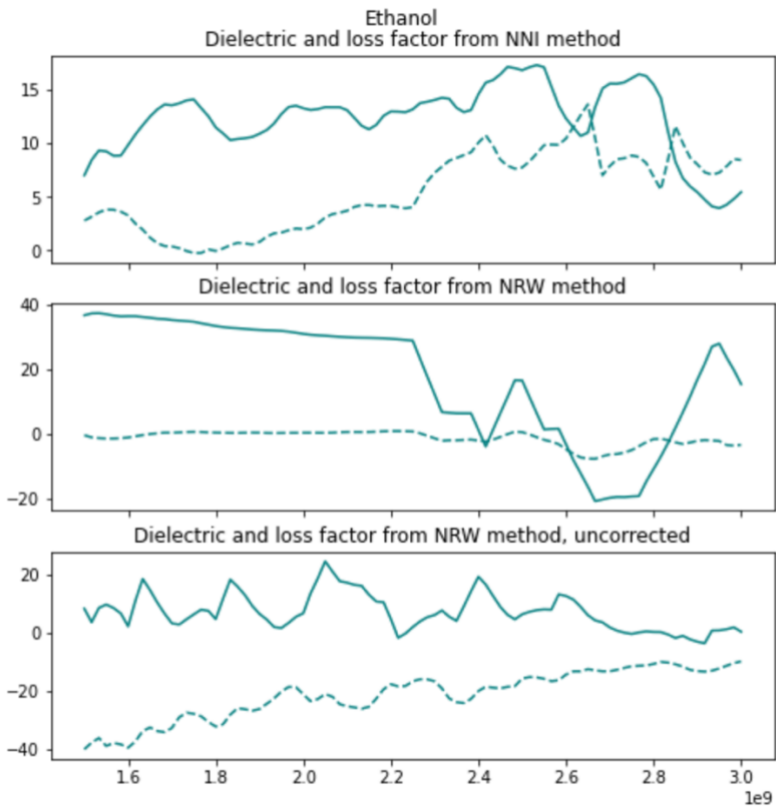
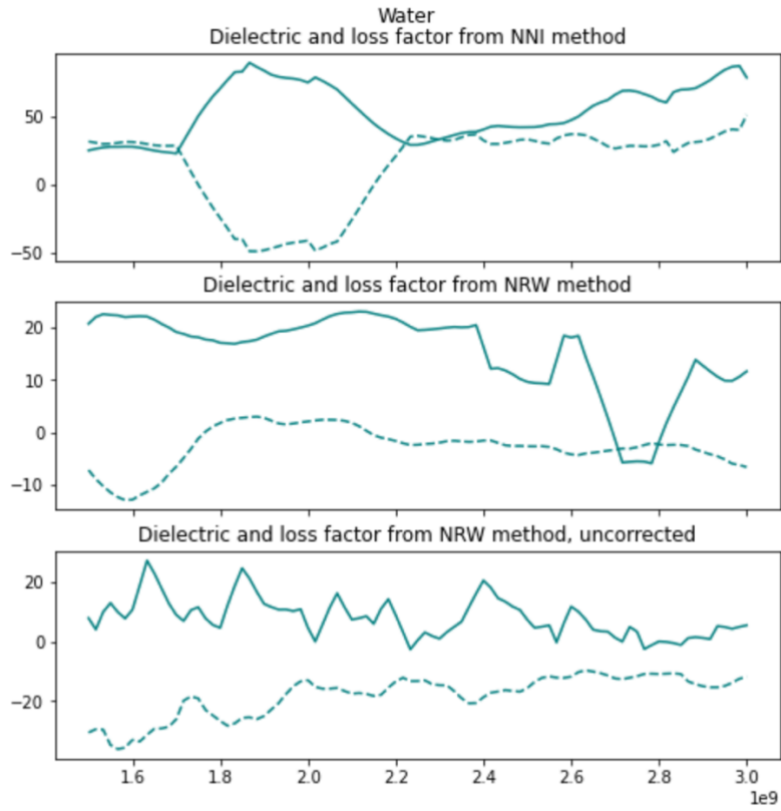
Now that we have our reflection and transmission coefficients, we need to get our complex permittivity out of them. This is more difficult than I assumed it would be! The procedure for this (I think) varies a bit on the testing set up you're using. It appears common to use an iterative method for this [13], but I tried using two non-iterative methods instead, the New Non-Iterative Method from [14] (abbreviated NNI), and Nicholson-Ross-Weir (NRW) [15]. The methodologies for both are described in [13], and in my implementation I leaned heavily on [this](#) implementation of NNI [16] and [this](#) implementation of NRW [13].

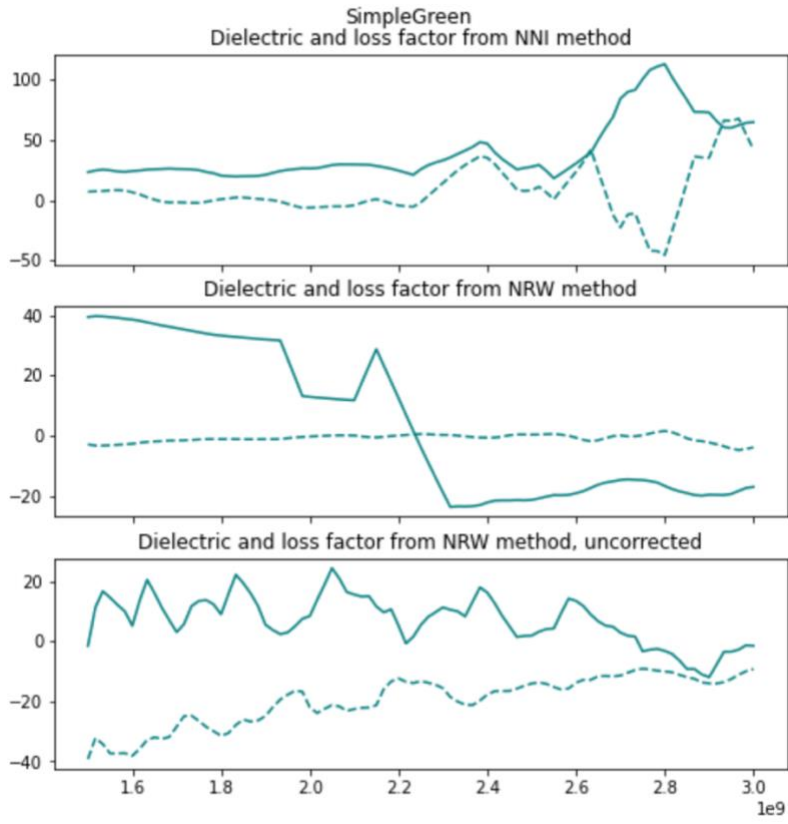
Results

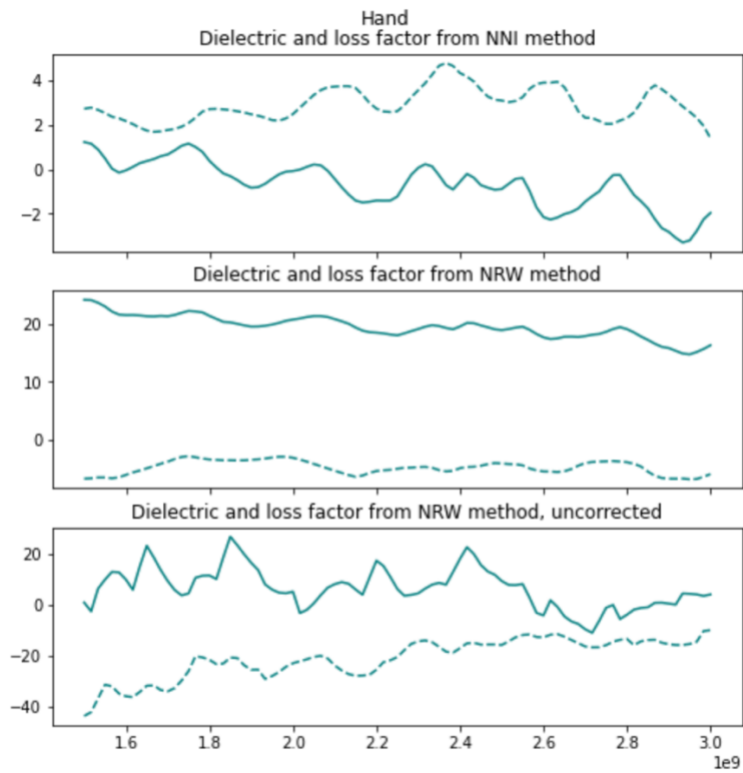
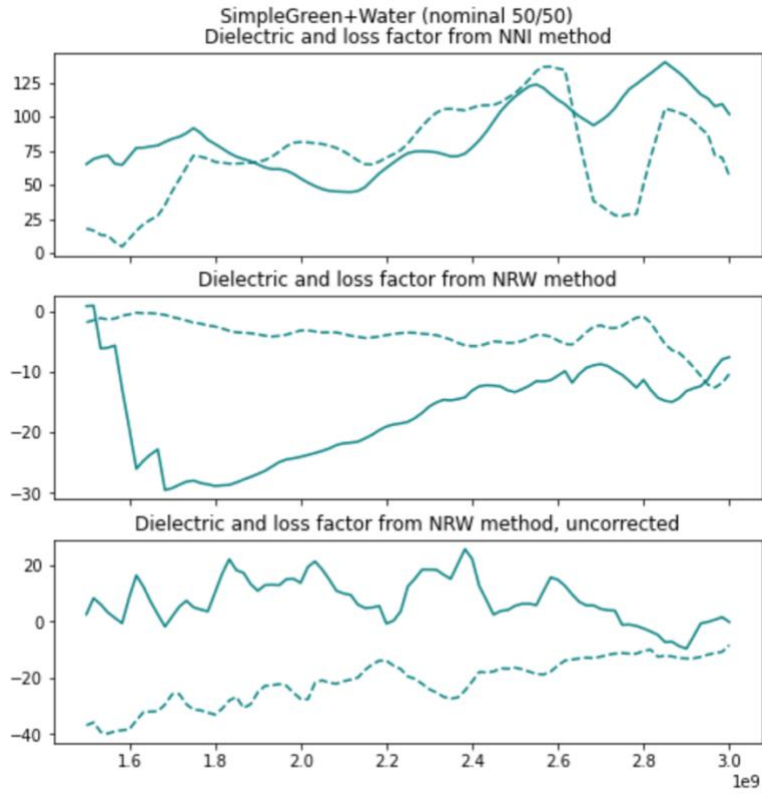
So, spoiler alert, the permittivity extraction did not go so well. Is it because of a problem in the physical apparatus? In the VNA calibration? In the TRL calibration? In the choice of permittivity extraction procedure? In the implementation of said procedure? I don't yet know! Though I suspect the answer could be any and all of them.

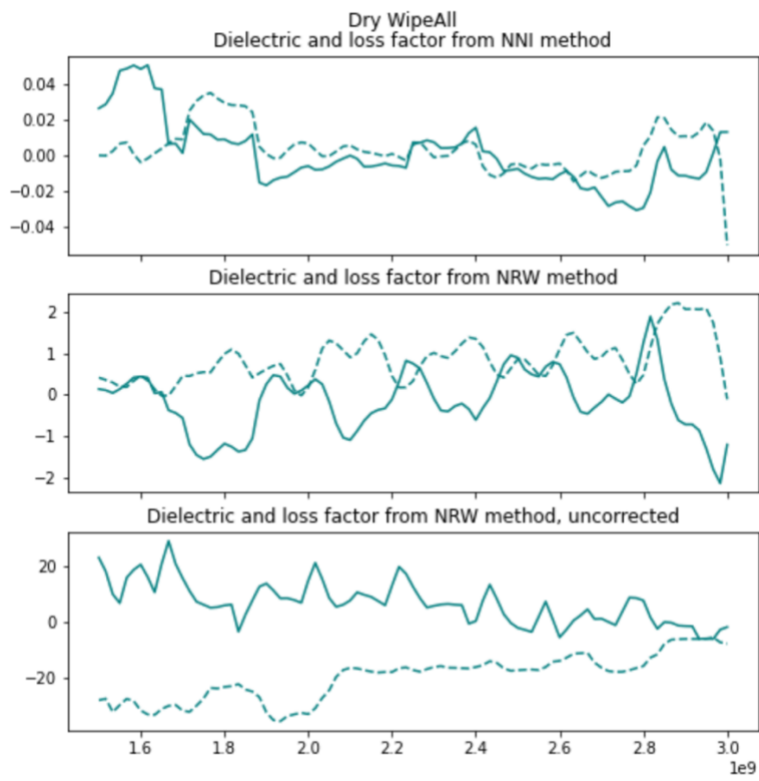
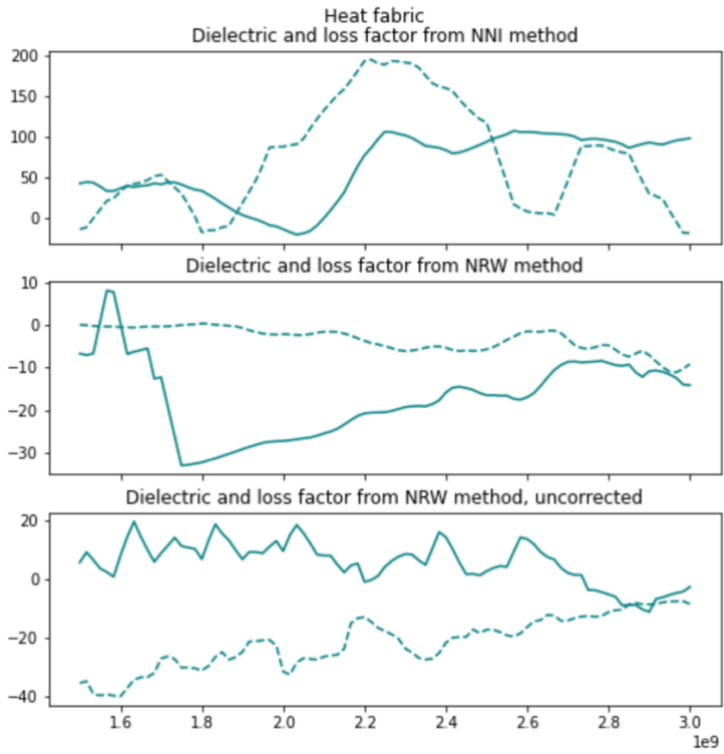
Permittivity

Here are all the permittivity measurements for the samples which it seemed mildly valid to do this with. I have plotted 3 versions of the permittivity for each, NNI, NRW, and NRW on the un-corrected data.









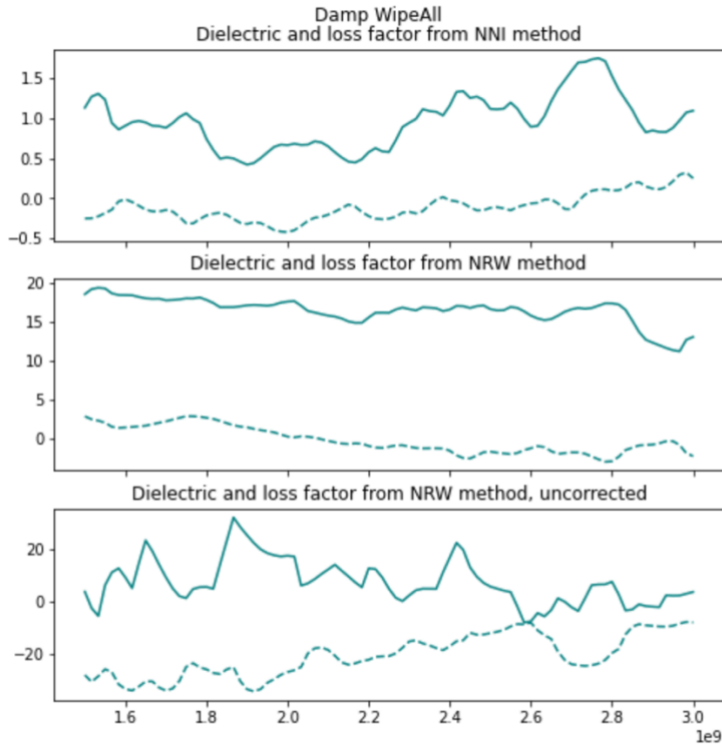
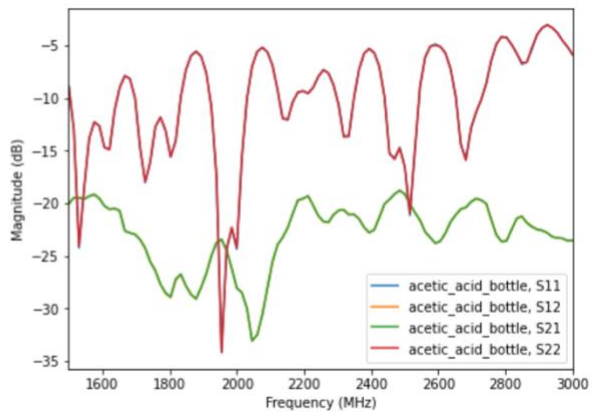
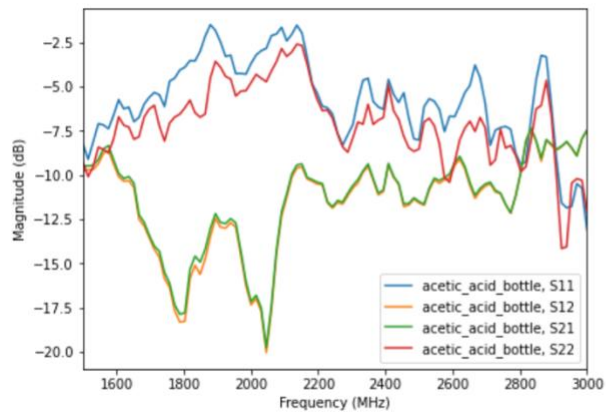
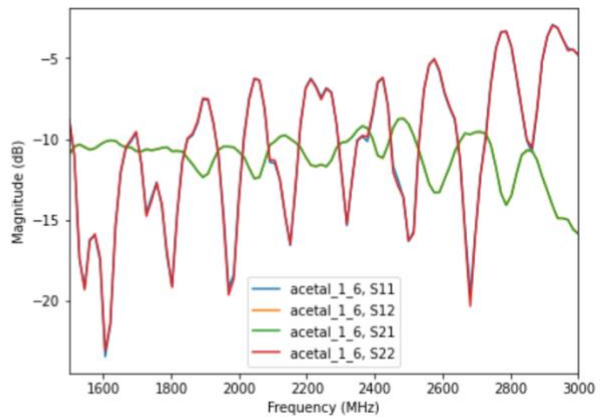
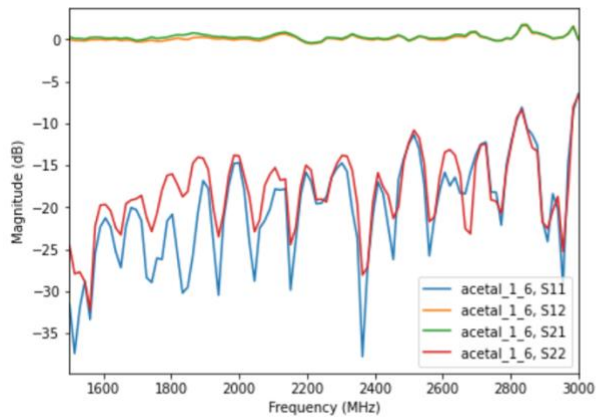
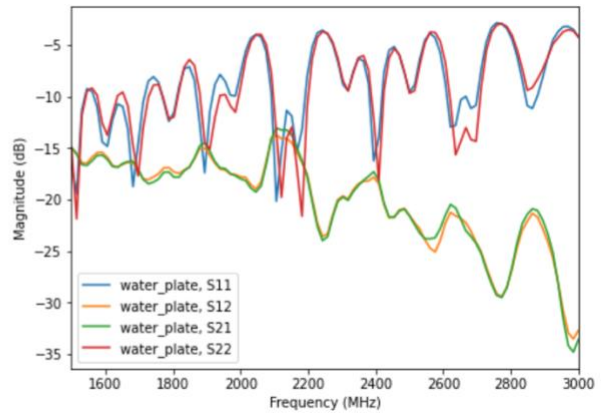
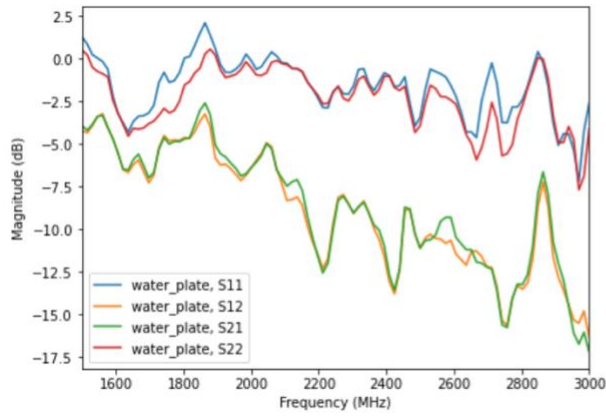


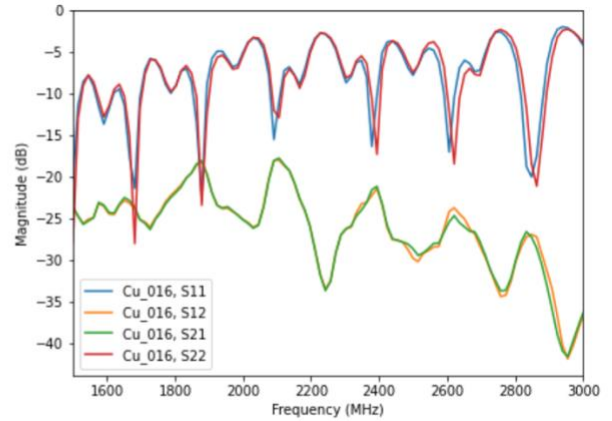
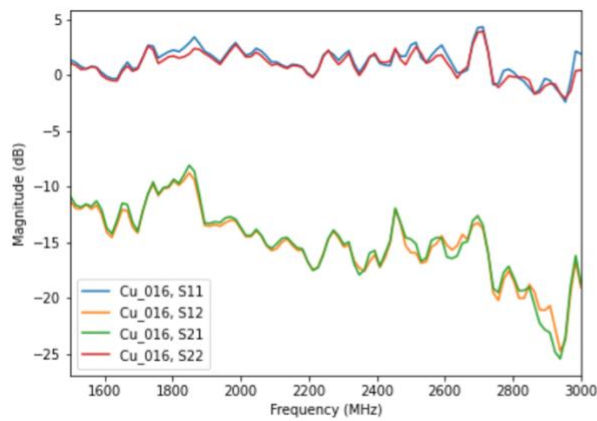
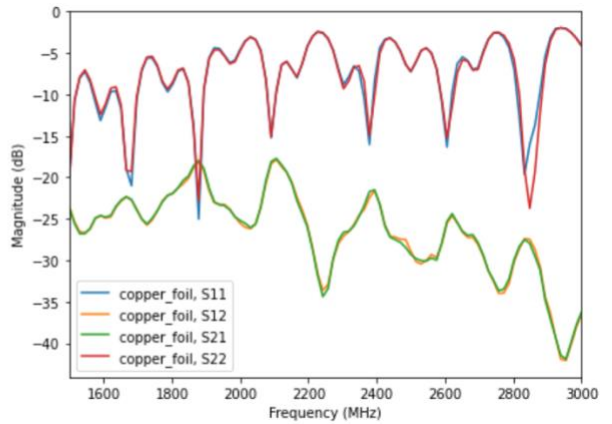
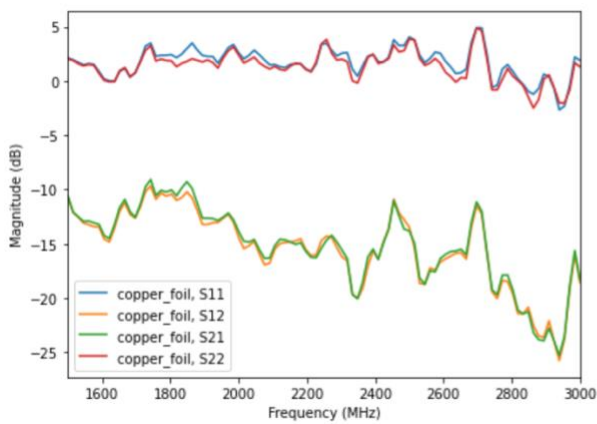
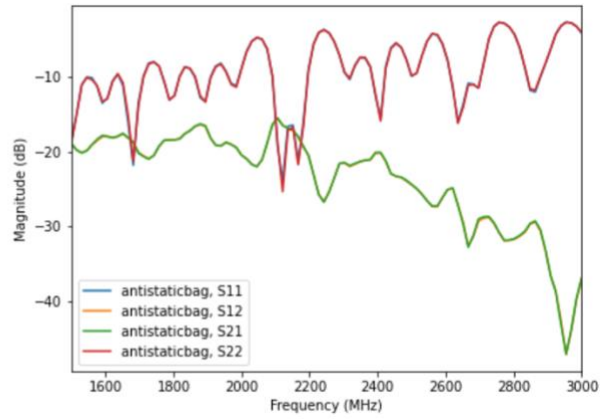
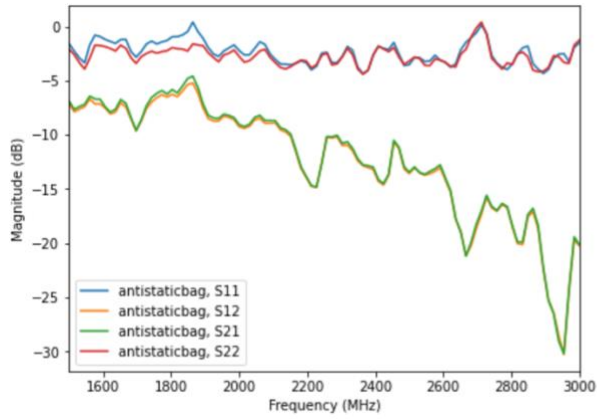
Figure 22 — Permittivity measurements. Solid line is ϵ' , dashed line is ϵ''

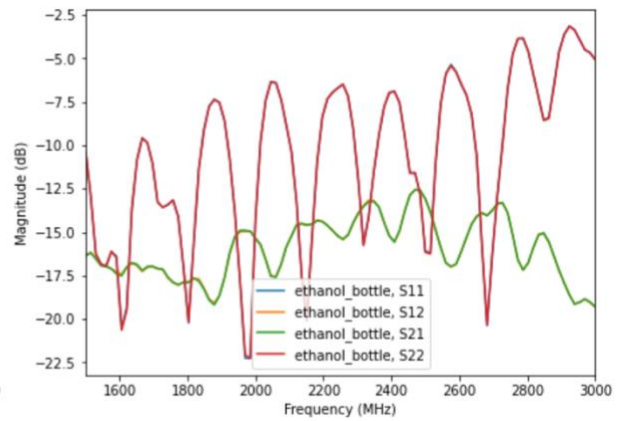
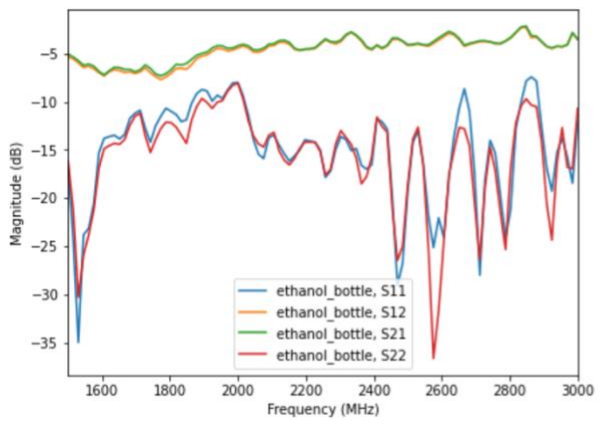
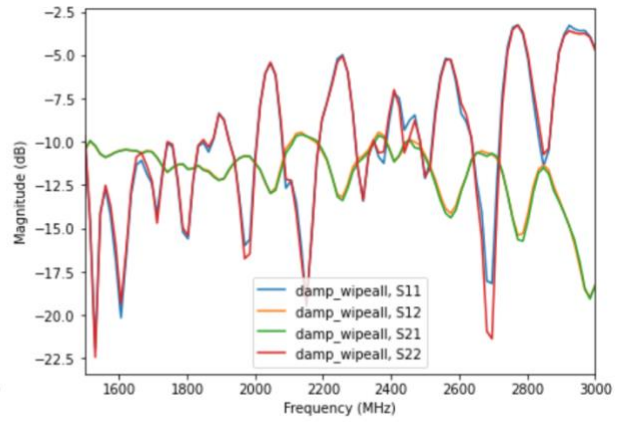
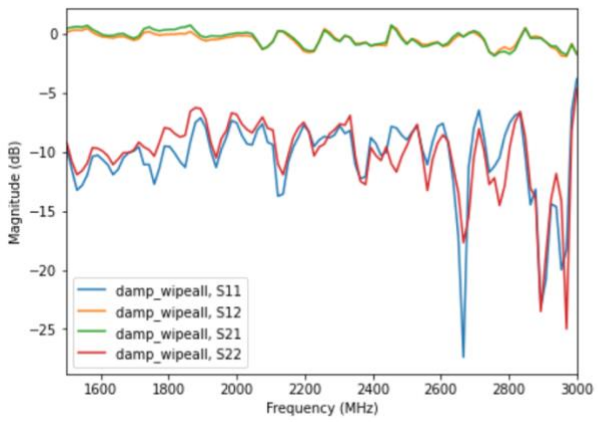
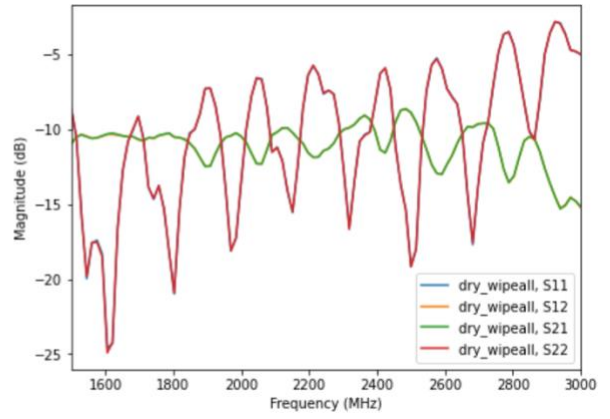
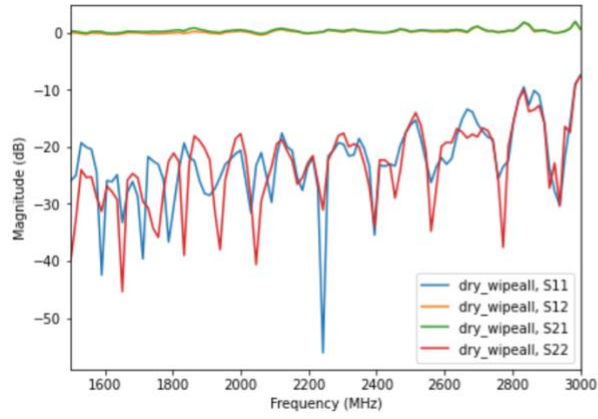
The NRW implementations have a recurrent not-non-negative problem. All the implementations are quite noisy; these are plotted with 10 sample moving average. All the implementations have what might be an offset problem. The other unfortunate thing about evaluating these is that in the frequency band that we're in, there aren't huge changes, which it makes it harder to see if we're in the right ballpark. Improving this goes into the beyond-the-scope-of-this-class-project bucket.

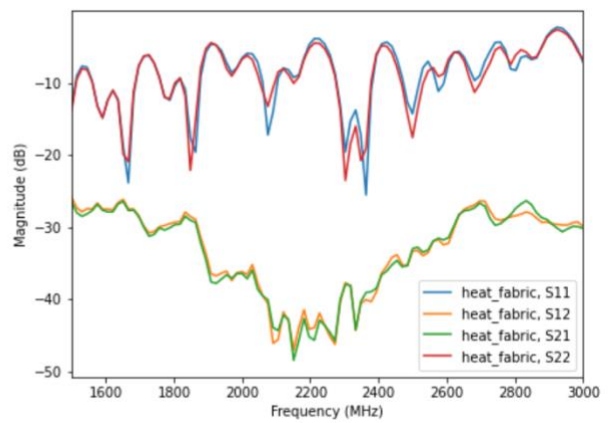
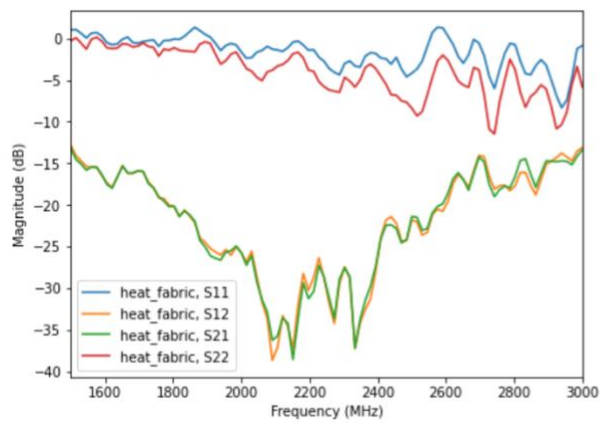
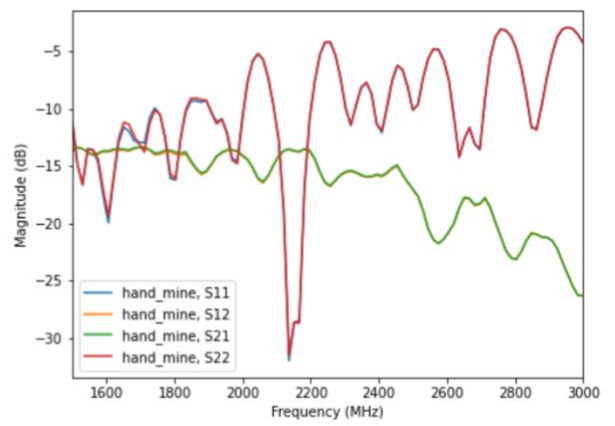
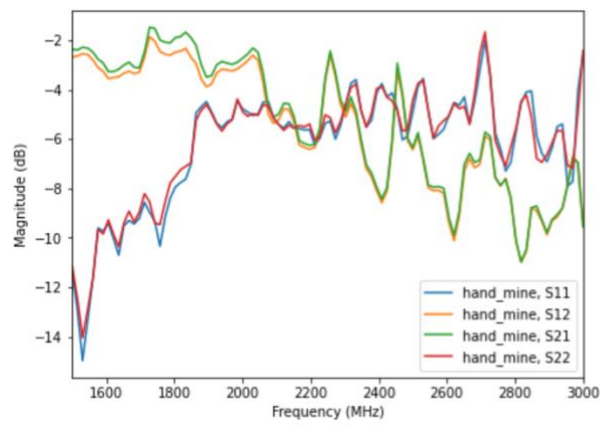
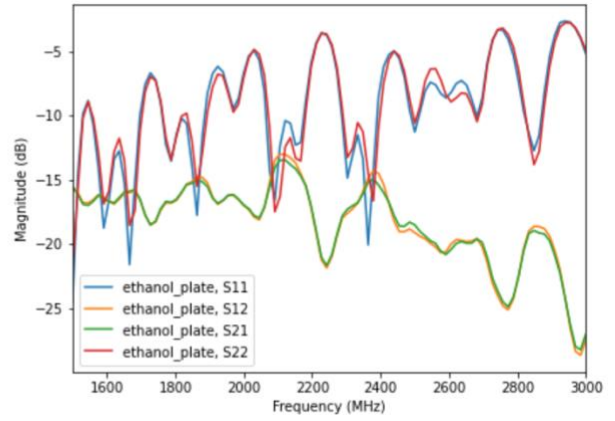
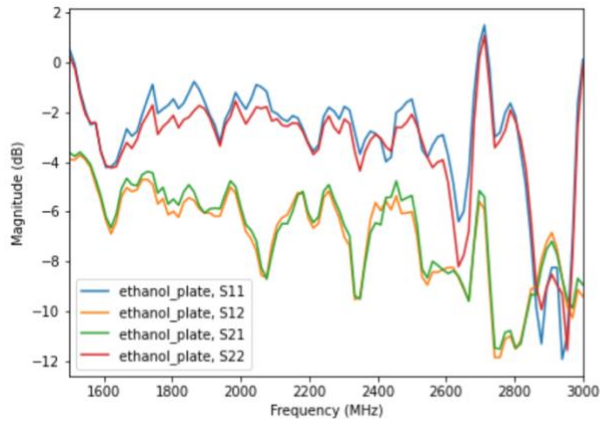
S-parameters, everything

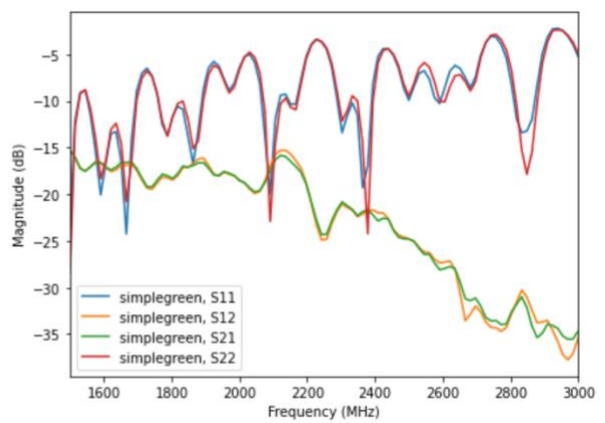
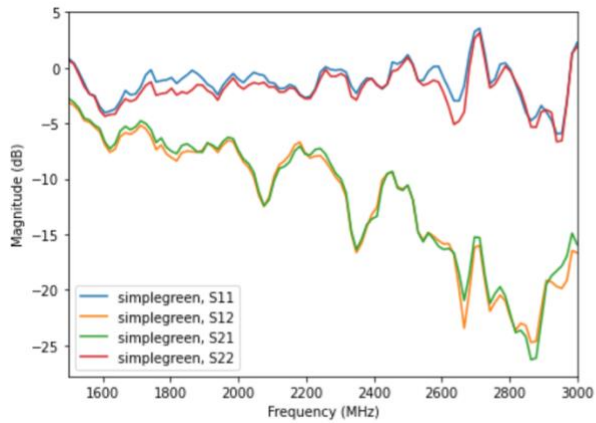
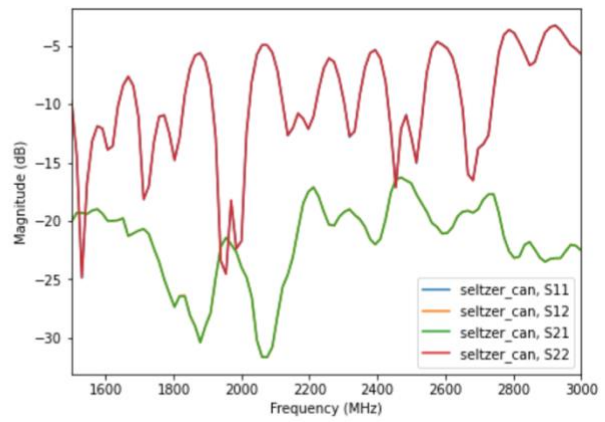
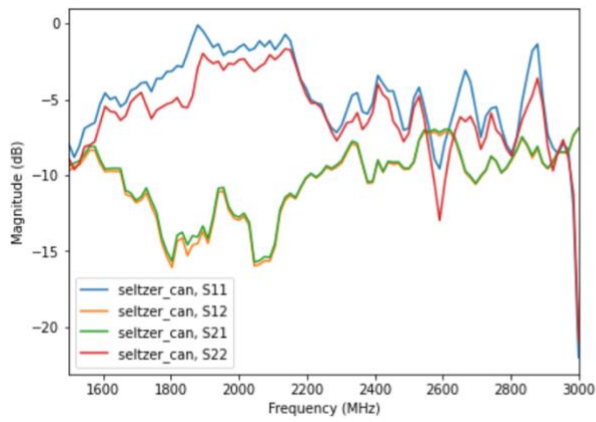
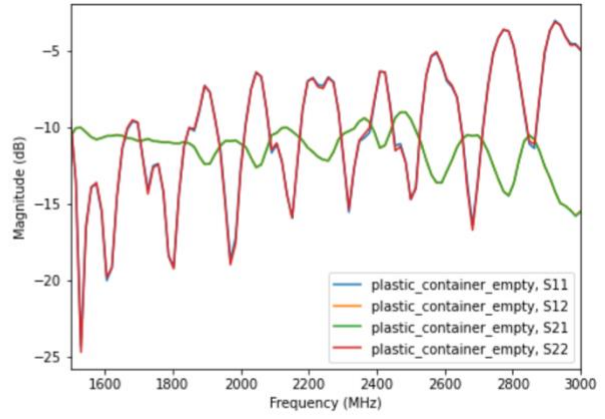
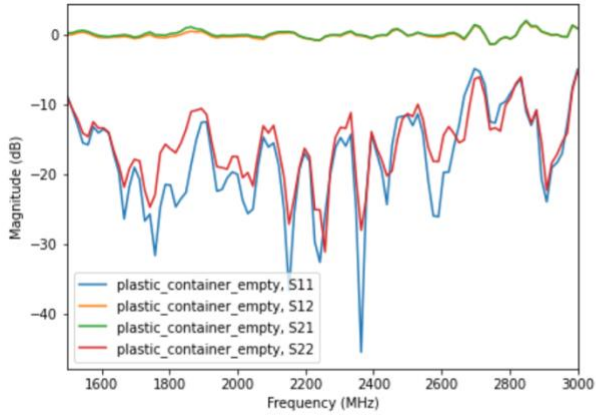
Here are the S-parameters (corrected and uncorrected) for every sample I measured. Some of these measurements are not of structures we would reasonably be able to get permittivity measurements out of! Some of these measurements I would think we could get permittivity measurement out of, and yet, can we?

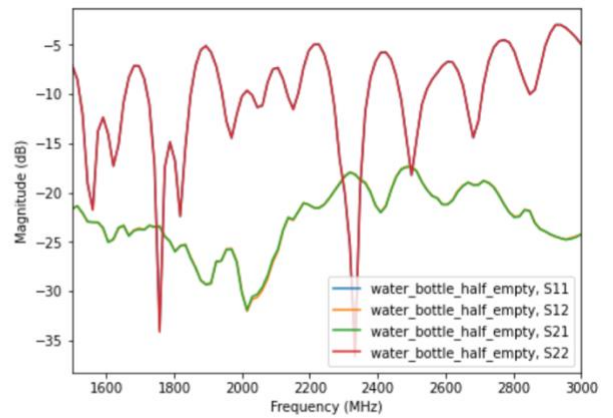
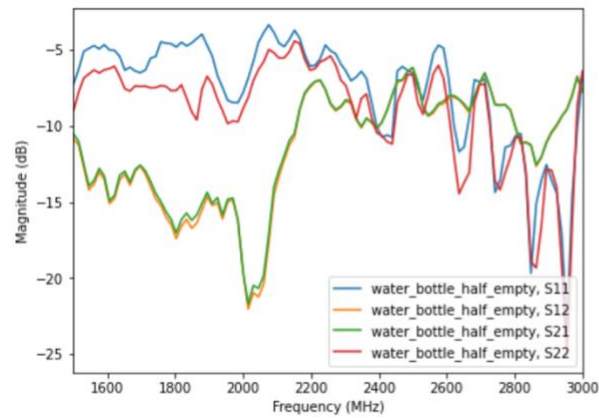
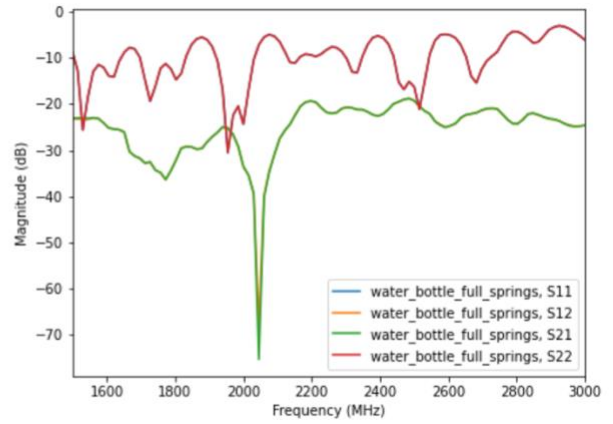
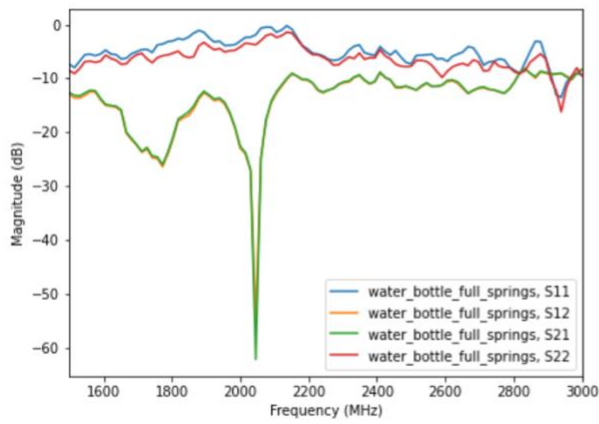
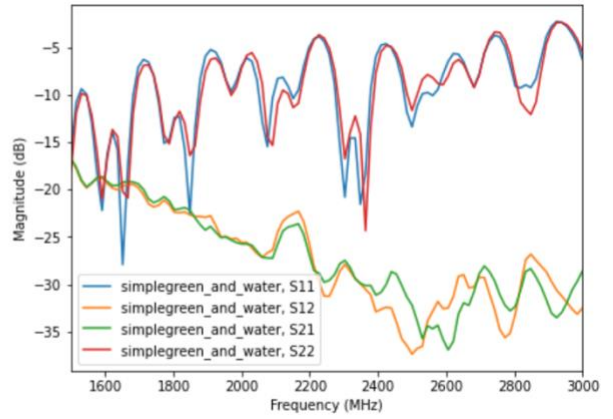
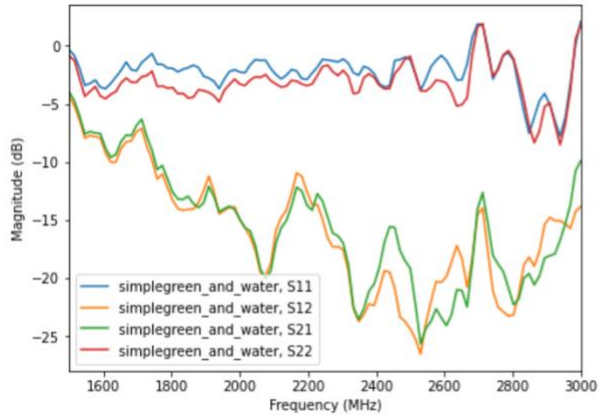












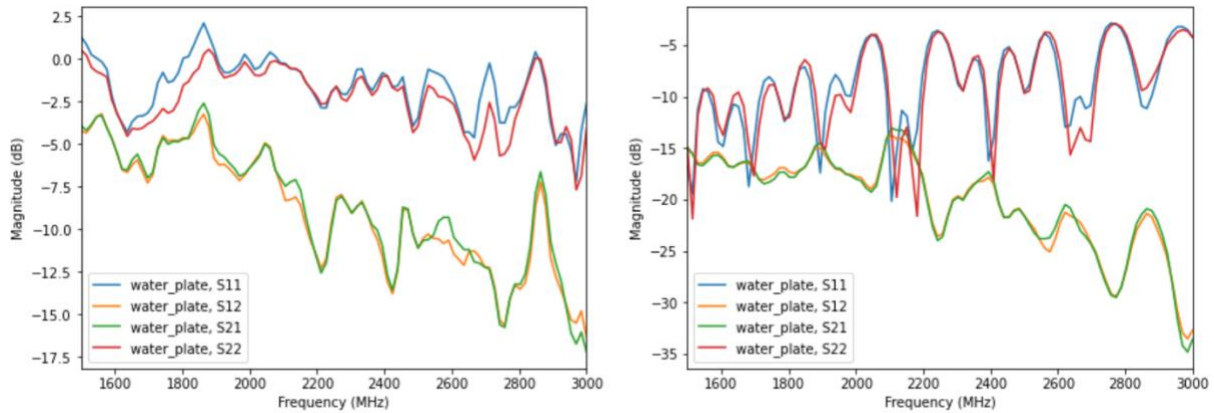


Figure 23 — All of the S-parameter measurements. Sample names are in the legend.

Summary

If the initial guiding question to this project is: “Can I do dielectric spectroscopy?” then the results of this project would suggest an ambivalent “maybe.”

I think someone with more experience in RF generally or dielectric spectroscopy specifically could make this project work and the output would be useful.

References

- [1] Agilent Technologies, “Basics of Measuring the Dielectric Properties of Materials”, Application Note. http://academy.cba.mit.edu/classes/input_devices/meas.pdf
- [2] Agilent Technologies, “Microwave Dielectric Spectroscopy Workshop – ‘Measure the Difference’”, presentation slides, 2004. http://academy.cba.mit.edu/classes/input_devices/DS.pdf
- [3] Woodward; Broadband Dielectric Spectroscopy: A Modern Analytical Technique ACS Symposium Series; American Chemical Society: Washington, DC, 2021. <https://pubs.acs.org/doi/pdf/10.1021/bk-2021-1375.ch001>
- [4] Brodie, Graham, Jacob, Mohan V. and Farrell, Peter. Microwave and Radio-Frequency Technologies in Agriculture: An Introduction for Agriculturalists and Engineers, Warsaw, Poland: De Gruyter Open Poland, 2015. <https://doi.org/10.1515/9783110455403>

- [5] Da Silva, Marco. (2022). Impedance Sensors for Fast Multiphase Flow Measurement and Imaging.
https://www.researchgate.net/publication/44229478_Impedance_Sensors_for_Fast_Multiphase_Flow_Measurement_and_Imaging
- [6] Analog IC Tips. WTW Media. 2022. Accessed May 17, 2022.
<https://www.analogictips.com/what-are-the-functions-and-principles-of-s-parameters-part-1/>
- [7] 3D Printing Your Own Antennas, Antennas Test Lab, 2021. Accessed May 17, 2022.
<https://antennatestlab.com/3dprinting>
- [8] Wade, P., “Rectangular Waveguide to Coax Transition Design”, QEX, 2006.
http://www.w1ghz.org/QEX/Rectangular_Waveguide_to_Coax_Transition_Design.pdf
- [9] NanoRFE User manual. Website. Accessed May 17, 2022.
<https://nanorfe.com/nanovna-v2-user-manual.html>
- [10] Engen, G. F., and Hoer, C. A., ““Thru–Reflect–Line”: An Improved Technique for”, 1979, IEEE Transactions Microwave Theory and Technique, Vol. MTT-27, No. 12.
<https://www.nist.gov/sites/default/files/documents/calibrations/mtt27-12.pdf>
- [11] Arsenovic et al., “scikit-rf: An Open Source Python Package for Microwave Network Creation, Analysis, and Calibration [Speaker’s Corner],” in IEEE Microwave Magazine, vol. 23, no. 1, pp. 98-105, Jan. 2022, doi: [10.1109/MMM.2021.3117139](https://doi.org/10.1109/MMM.2021.3117139).
- [12] R.B. Marks, “Formulations of the Basic Vector Network Analyzer Error Model including Switch-Terms,” in ARFTG Conference Digest-Fall, 50th, 1997, vol. 32, pp. 115-126
- [13] Kintner, C. E. (2017). Free-Space Measurements of Dielectrics and Three-Dimensional Periodic Metamaterials. Graduate Theses and Dissertations Retrieved from <https://scholarworks.uark.edu/etd/2557>
- [14] Boughriet, A. H., Legrand, C., & Chapoton, A. (1997). Noniterative stable transmission/reflection method for low-loss material complex permittivity determination. IEEE Transactions on Microwave Theory and Techniques, 45(1), 52–57. <http://doi.org/10.1109/22.552032>
<https://ieeexplore.ieee.org/stamp/stamp.jsp?tp=&arnumber=552032>

[15] Nicolson, A. M., & Ross, G. F. (1970). Measurement of the Intrinsic Properties of Materials by Time-Domain Techniques. *IEEE Transactions on Instrumentation and Measurement*, 19(4), 377–382. <http://doi.org/10.1109/TIM.1970.4313932>

[16] Boivin, A. “permittivitycalc” (2019). <https://permittivitycalc.readthedocs.io/en/stable/index.html#boughriet1997>. Accessed May 17, 2022.

Additional readings/references

1. https://indico.cern.ch/event/897769/contributions/3786083/attachments/2002987/3376768/Broadband_Dielectric_Spectroscopy.pdf
2. https://www.researchgate.net/publication/228980557_An_overview_of_microwave_techniques_for_the_efficient_measurement_of_food_materials
3. <https://www.mdpi.com/1424-8220/21/10/3321/htm>
4. https://www.researchgate.net/publication/292156806_Comparative_Study_of_Materials_Characterization_using_Microwave_Resonators
5. <https://www.pasternack.com/wr-430-waveguide-standard-gain-horn-antenna-15-db-sma-pe9864b-sf-15-p.aspx>
6. <https://www.semanticscholar.org/paper/Development-of-Complex-Relative-Permittivity-System-Tosaka-Fujii/b71cf27673917eaaf8f4a38a4539cce69972d2d8>
7. <https://www.electronics-notes.com/articles/antennas-propagation/horn-antenna/theory-equations.php>
8. <https://pubs.rsc.org/en/content/articlelanding/2014/cp/c3cp55272a>
9. http://emlab.uiuc.edu/ece451/appnotes/new_TRL.pdf
10. https://zone.ni.com/reference/en-XX/help/373153D-01/vnahelp/calibration_trl/#:~:text=TRL%20is%20one%20type%20in,the%20following%20necessary%20calibration%20standards.
11. <https://nvlpubs.nist.gov/nistpubs/Legacy/TN/nbstechnicalnote1536.pdf>
12. <https://ieeexplore.ieee.org/stamp/stamp.jsp?tp=&arnumber=6229351>